Butanol and gasoline-like blend combustion characteristics for injection conditions of gasoline compression ignition combustion mode

Tung Lam Nguyen, Camille Hespel, Dinh Long Hoang, Christine Mounaïm-Rousselle

Butanol and gasoline-like blend combustion characteristics for injection conditions of Gasoline Compression Ignition combustion mode

Tung Lam Nguyen[*a,b] , Camille Hespel[a], Dinh Long Hoang[c], Christine Mounaïm-Rousselle[a]

[a] Univ. Orléans, INSA CVL, PRISME, EA 4229F45072 Orléans, France

[b] Univ. Transport and Communications, Hanoi 117200, Vietnam.

[c] Hanoi Univ. Science and Technology, Hanoi 113400, Viet Nam

Corresponding and Contact Author:

Tung Lam Nguyen

Université d'Orléans- Laboratoire PRISME

Polytech Orléans

8 rue Léonard de Vinci, 45072 – Orléans Cedex 1

Phone: +33-02-38-49-47-28

Fax.: +33-02-38-41-73-83

Email: tung-lam.nguyen@etu.univ-orleans.fr and lamnt@utc.edu.vn

Submitted for consideration at the Fuel journal.

Abstract

As bio-butanol would be one promising alternative fuel to mitigate the energy crisis and reduce the environmental impact of the automotive sector, its potential as blend in gasoline has been widely evaluated especially for conventional Spark Ignition engines. But recent studies prove that Gasoline Compression Ignition operating mode could be a future interesting advanced combustion mode to reach higher efficiency and lower pollutant emissions than conventional SI engines. The objective of this paper is to underline the effect of butanol blend in gasoline in injections conditions needed in GCI by set experimental study in a High Pressure/ High Temperature chamber. Therefore, first data about sprays and combustion characteristics as a function of the butanol content in a gasoline surrogate (PRF80) at injection conditions of GCI, i.e. high pressure (6 MPa) and high-temperature (900 K) conditions but with injection pressure of 40 MPa are given and he results discussed thanks to kinetics simulation of ignition delays.

Keywords: n-butanol/PRF80 blend, Spray and Combustion Characterization, Flame Lift-Off Length, Ignition Delay.

1. Introduction

We are now aware that global energy resources and environmental impacts are major issues for the future of our society. Concerns over future petroleum supply and environmental degradation from fossil fuels have led to substantial interest in the production and use of biomass-derived fuels, due to their global impact on CO_2 production. Second-generation biofuels, manufactured from various types of biomass (wood, plant waste, and more generally lignocellulose material) are superior to the first generation, from food crops (i.e. ethanol and biodiesel) in terms of energy balance, reduction of greenhouse gas emissions and food security. Bio-butanol is one of these second-generation biofuels, well suited for Internal Combustion Engines due to its similar physical properties to engine fuel. In comparison with ethanol, n-butanol is more compatible with existing engines when blended with conventional gasoline or diesel fuels, thus avoiding phase separation and increasing cost-effectiveness in the transportation infrastructure [1].

Even if the CO_2 impact of Compression Ignition (CI) engines is lower than that of Spark Ignition (SI) engines due to their higher efficiency, NOx and soot emissions remain an important drawback as stringent emission legislation demands a continued reduction in engine-out emissions. Therefore, over the last few decades, several advanced combustion concepts based on low temperature combustion have been introduced in order to reduce pollutant emissions from CI engines. As example, Homogeneous Charge Compression Ignition (HCCI), characterized by spontaneous auto-ignition of a lean premixed fuel/air mixture, allows ultra-low NO_x and soot emissions compared to the traditional diesel combustion mode. But it has some disadvantages such as: (1) difficulty controlling HCCI combustion as the auto-ignition process depends on pressure, temperature, O_2 concentration, diluent and fuel properties; (2) high acoustic noise at high loads; (3) high HC and CO emissions at low loads.

To overcome the limitations of the CI and HCCI combustion modes, some other combustion concepts, such as Partially Premixed Combustion (PPC), have been developed. By replacing the strongly reactive fuel, i.e. diesel type, by a less reactive one, i.e. gasoline type, emissions can be drastically reduced [2–7]. Gasoline Compression Ignition is a potential strategy to achieve high specific power, high fuel efficiency, as well as low soot and NO_x emissions. The reduction of the temperature inside the cylinder and the ignition delay time extension are two ways to achieve PPC as an advanced combustion method, offering low NO_x and soot emissions. Dempsey et al. [8] provided recently an interesting analysis about the effect of stratification process obtained by different multiple-injection strategies on the emission (NO_x/HC/CO and smoke) and engine performance. They reminded that due to its longer ignition delay, gasoline like fuels allows a better mixing in the cylinder with the ambient air prior the combustion. Thanks to multiple-injection strategy, a portion of the fuel is well “premixed” with air and the post-injection timing allows the control of the start of ignition or combustion. Labreche et al. [9] studied the effect of the second injection phasing and concluded that even if the first injection is early, the second one has to be adjusted near the

Top Dead Center (TDC), so the fuel is injected in conditions similar to Conventional Diesel Combustion but due to the physical specificities of gasoline type fuel, the injection pressure has to be adjusted, as confirmed in [10].

Manente et al. [11] explored the impact of the octane number range from 70 to 100 on the optimization of GCI combustion. They concluded their study by the suggestion that the change of chemistry affects more the combustion and the pollutant emissions than the mixing itself. Cung et al. [12] studied also the effect of three different type of gasoline fuels with different chemical composition but similar RON (Research Octane Number). Most of studies done about alcohols fuel in GCI combustion modes concern ethanol as in [13–16], with a positive effect on soot emission and also the confirmation that the best injection strategy remains the double injection one as in [17]. But only few studies are focused on the possibility to use butanol blend for GCI applications. As example, in [18], the first investigation indicated also that adding n-butanol improves the oxidation of CO and HC emissions slightly, but with not really NO_x emissions. Yang et al. [19] studied also the combined effects of EGR and adding n-butanol to improve soot emissions. But butanol offers many advantages in comparison to ethanol due to its physical and chemical specificities as its lower vaporization heat, higher miscibility with gasoline, higher cetane number ….

More studies are carried out about the effect of butanol addition to gasoline surrogates on the auto-ignition process without consider the mixing processes as in a constant volume combustion device and homogeneous charge compression ignition engine [20], or a shock tube [21] or in rapid compression machine [22]. But the lack of studies and data available on the butanol addition effect on the spray/combustion characteristics under GCI conditions as done in [23] for gasoline suggested the present study.

Therefore, the objective of this study was to carry out experiments in a High-Pressure/High-Temperature facility to characterize the effect of n-butanol on the spray and combustion processes for different butanol-PRF80 blends by considering the second injection conditions as in GCI combustion mode. For that, as the optimized condition was found near Top Dead Center, the standard conditions, defined by Engine Combustion Network (https://ecn.sandia.gov/), are considered (900 K ambient temperature and 6 MPa ambient pressure, i.e. Spray A) but with a lower injection pressure (40 MPa). The impact of butanol blend on liquid and vapor spray penetration, the ignition delay and the flame lift-off length is given for the first time to provide dataset to improve future modelling works. Some results from autoignition computations based on a detailed kinetic mechanism are provided to help the discussion about the impact of n-butanol in these conditions.

2. Experimental approach

2.1 Experimental facility

The High-Pressure/High-Temperature vessel, called NOSE (New One Shot Engine) is fully described in [24,25]. It is based on a single cylinder engine (155 mm bore diameter and 177.8 mm stroke), driven by an electric motor (Figure 1). The

revolution speed of the electric motor is controlled as a function of the crank angle to obtain a plateau near the TDC with constant thermodynamic conditions. The combustion chamber was designed to support optical measurements.

The working mode of NOSE starts by setting the initial conditions (pressure and temperature) and intake ambient gas composition. So, after creating a vacuum, different gases (N_2 or N_2/O_2) are injected into the chamber thanks to a mass flow controller (Brooks instruments). The initial temperature is specified by controlling the temperature of the water around the liner and of four heaters located in the cylinder head and set at 90 °C ± 0.5 °C. Two type-K thermocouples are installed inside the chamber and near the injector to measure the gas temperature inside the chamber and the casing temperature, respectively to control the temperature of the chamber and of the ambient gases before injection and combustion. In [25], the homogeneity of the temperature field was verified at different locations in order to validate this set-up as ECN standard set-up A high frequency piezo-electric pressure sensor (KISTLER 7001) is installed at the chamber head and is coupled to a charge amplifier (KISTLER 5011).

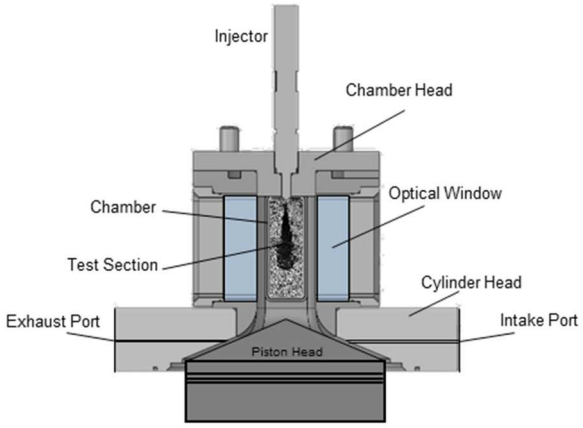

Figure 1. The NOSE chamber: cross-section view

The cylinder pressure, temperature inside the vessel, driven current of the injector, photomultiplier signal and crank angle are recorded as a function of time with a National Instruments CompactRIO at 250 kHz. The injection system consists of the following components: (1) a high pressure pneumatic pump, (2) a high pressure line, and (3) a common rail. The respective fuel for each test was provided to the injection by a high pressure pneumatic pump MAXIMATOR M189 DVE-HD driven by an air piston pump to maintain pressure before injection, controlled by a PID system with a pressure regulator.

The single-hole CRI 2.16 Bosch was used as ECN Spray A specification. The nozzle was 0.0885 mm in diameter and the k-factor was 1.5. The nozzle tip of the fuel injector was held at a constant temperature of 363 K by circulating coolant during operation. The injection duration was set to 3 ms. In the case of inert conditions, 100% N_2 was introduced to prevent ignition and for reactive conditions an oxygen molar fraction of 21% was added. The injection pressure of 400 bar was based on previous studies about Gasoline Compression Ignition [7,10].

This experimental facility achieve High-Pressure/High-Temperature conditions with a high repeatability. The

observed shot-to-shot variations are respectively 1.6%, 1%, 0.5%, 4.5% and 5% for ambient temperature, ambient pressure, oxygen rate, density and injection pressure. According to the models used in the manuscript, its variations imply an accuracy of 5%, 8%, 13% and 8% for the measurement of liquid penetration, vapour penetration, lift-of length and ignition delay respectively.

2.2 Measurement techniques

The optical techniques set up around the NOSE chamber were fully described in [24]. These techniques are based on ECN requirements with signal processing tools. Table 1 summarizes the optical setup for both inert and reactive atmosphere to characterize macroscopic combustion parameters. Figure 2 shows the scheme of the optical setup for reactive conditions.

Table 1. Summary of the optical setup

	Inert atmosphere		Reactive atmosphere	
Studied Parameters	Liquid length	Vapor Spray	Ignition delay	Lift off length
Optical Technique	DBI	Schlieren	OH* Chemilu.	OH* Chemilu.
Camera/ Detector	Phantom - V1611		Newport PMT 70680	Photron - APX-I2
Sensor type	CMOS		PM	ICCD
Light source	LED plate	LED	-	-
Lens/ Mirrors	60 mm (f/2.8)	2 Parabolic Mirrors (34 inches diameter) Pinhole of 6 mm	-	UV 60 mm (f/3.5)
Pin hole (mm)		6	-	-
Filter	-	-	BPF 307 nm FWHM 10 nm	BPF 310 nm FWHM 10 mm
Frame speed (kHz)	49	39	2	39
Exposure time (µs)	3	5	-	499
Image size (pi^2)	512 x 384	1024 x 400	-	512 x 1024
Magnification (pix/mm)	12	12.3	-	18.2

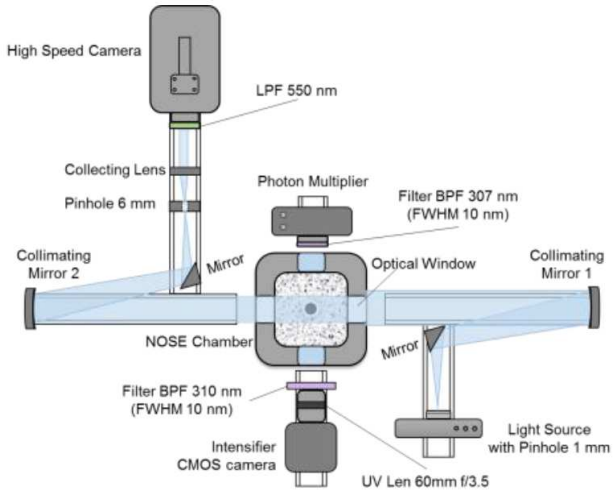

Figure 2. Scheme of optical setup for reactive atmosphere

Some images or signals obtained from these different techniques are plotted in the following sections to illustrate the quality of the set-ups.

2.3 Fuels

As the objective of this study is to provide data and some understanding about the effect of blending butanol in gasoline in the Gasoline Compression Ignition mode, PRF80 was chosen as the gasoline surrogate and different quantities of butanol in volume were added with an increment of 20%, denoted Bu0, Bu20, Bu40, Bu60. The main properties of the pure fuels and blends are given in Table 2. The properties of the blends were estimated by weighted the value of each single component with its volumetric fraction. Viscosity of pure n-heptane, iso-octane, n-butanol and all blends was measured by viscosity meter. As expected due to the pure butanol properties, the increase of butanol amount increases the density and viscosity while the lower heating value decreases. This should be considered to supply the same amount of chemical energy.

Several studies have been carried out to identify the best way to estimate the Research Octane Number for alcohol and gasoline mixtures [26,27]. Because of the higher molecular weight of butanol, closer to that of gasoline, their molar and volumetric concentrations are similar, and there is no significant difference in blend octane number estimations for these compounds using volumetric or molar concentrations. The research octane number (RON_{blend}) of n-butanol blends was calculated by RON prediction of a linear molar-weighted model [26] given by:

$$RON_{blend} = (1\text{-}x_{mole}).RON_{PRF80} + x_{mol}.RON_{n\text{-}bu} \qquad \text{Eq. 1}$$

in which: $RON_{PRF80} = (1\text{-}y_{mole}).RON_{iso\text{-}octane} + y_{mol}.RON_{n\text{-}heptane}$, where x_{mol} is the molar fraction of n-butanol in the blend; y_{mol} is the molar fraction of n-heptane in PRF80. One effect of the addition of n-butanol as in Table 2, is the decrease of the reactivity quality as predicted the estimate of the RON by Eq.1, which is important in the case of PPC combustion mode. Moreover, its higher evaporative cooling effect than gasoline also contributes to increase the ignition delay.

143 *Table 2. Fuel properties of Primary reference fuels*

Properties	n-heptane	iso-octane	PRF80	n-butanol	Bu20	Bu40	Bu60
Molecular formula	C_7H_{16}	C_8H_{18}	$C_{7.8}H_{17.6}$	C_4H_9OH	$C_{7.04}H_{15.88}$--$(OH)_{0.2}$	$C_{6.28}H_{14.16}$--$(OH)_{0.4}$	$C_{5.52}H_{12.44}$--$(OH)_{0.6}$
M_f, Molar weight [g.mol^{-1}]	100	114	11.2	74	103.76	96.32	88.88
Oxygen content [%]	-	-	-	21.6	3.08	6.64	10.8
ρ_f, Density at 15 ºC [kg.dm^{-3}]	0.684	0.692	0.6904	0.8098	0.718	0.742	0.765
υ_f, Viscosity at 15 ºC [mm^2.s^{-1}]	0.344	0.504	0.452	4.142	0.705	1.212	1.901
υ_f, Viscosity at 40 ºC [mm^2.s^{-1}]	0.214	0.336	0.268	2.211	0.451	0.724	1.050
υ_f, Viscosity at 70 ºC [mm^2.s^{-1}]	0.014	0.144	0.065	1.130	0.205	0.318	0.472
LHV, Lower heating value [MJ.kg^{-1}]	44.6	44.3	44.36	33.1	42.11	39.86	37.60
L_v, Latent heat of vaporization at 298 K [kJ.mol^{-1}]	31.6	31.01	31.13	43.07	33.52	35.90	38.29
Air-fuel stoichiometric (mass) ratio	15.14	15.09	15.10	11.21	14.32	13.54	12.77
RON (linear molar-weighted model)	0	100	80	96	83.2	86.6	89.6
Boiling point at 1 atm [ºC]	98.38	99.3		117.8			
P_v, Vapor pressure at 298 K [kPa]	4.6	5.5		0.58			
Auto-ignition temperature [◦C]	220	396		343			
c_{pf}, Specific heat at 15 ºC [kJ/kg.K]	2.24	2.05		2.39			

144 ***2.4 Mass flow rates for blends***

145 The physical parameters of the different blends can affect the global injected fuel quantity. For that, the average mass
146 flow rate (MFR) for the injection conditions (i.e. ambient and injection pressures of 60 bar and 400 bar respectively) was
147 measured thanks to an IAV Injection rate system (model K-025-50). As example, in Figure 3, the results of the average from
148 20 repetitive injections with an injection duration of 3 ms are presented for the maximum of Butanol content, i.e. 60% in vol.,
149 in comparison to PRF80. First, the initial hydraulic delay is not affected by the fuel difference, contrary to the final hydraulic
150 one, longer in the case of Bu60. Second, the quantity of fuel injected is slightly higher in the case of Bu60 denser than PRF80.

Indeed, the discharge coefficient, C_d estimated as the ratio between the average MFR [3 ms – 4 ms] and the theoretical one is equal to 0.86 for these two fuels. Therefore, the energy input corresponding is 317 kJ and 300 kJ for PRF80 and Bu60 respectively.

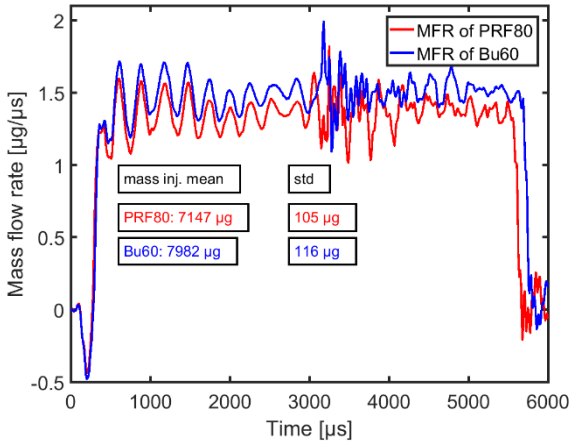

Figure 3. Mass flow rate for PRF80 and Bu60

2.5 Analysis tools

- **From the in-cylinder pressure signal**

From the in-cylinder pressure signal, filtered with a low-pass filter, first the heat release rate (HRR) was estimated by a simple estimate of the wall-heat transfer (in order to get HRR = 0 before injection timing): $\frac{dQ}{dt} = \frac{\gamma}{\gamma-1}.P.\frac{dV}{dt} + \frac{1}{\gamma-1}.V.\frac{dP}{dt}$, with P and V the combustion vessel pressure and volume respectively. As the air was assumed as the main component of the ambient, so the isentropic ratio, γ is only function of temperature. For that, the correlation of the specific heat as a function of temperature from [26] was used, with the average temperature estimated where the inlet valve closed was set at TDC.

This estimate helps to identify different phases of the combustion as the start of combustion (SOC), the premixed combustion and the late mixing controlled combustion phase. The ignition delay, ID, is then the time interval between the start of injection, SOI, and SOC. But as SOC is not absolute, i.e. low pressure or HRR gradient, it was also estimated by means of optical techniques as Schlieren imaging images or OH* time-resolved chemiluminescence.

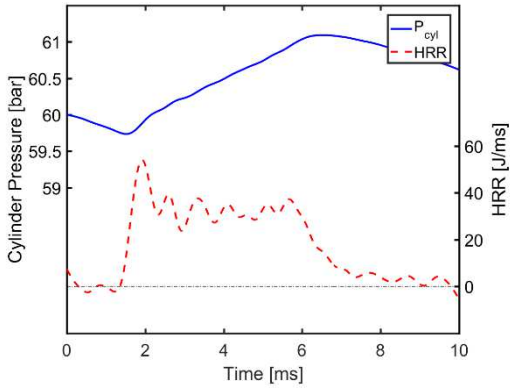

Figure 4. Typical cylinder pressure and heat release rate

To globally characterize the combustion development, BMF (Burned Mass Fraction) 10/50/90 are defined as the time durations where 10/50/90% of the heat has been released, as done for engine combustion analysis. From that, the Combustion Duration, CD, is defined as the difference between BMF90 and BMF10, i.e. the time in which 10-90% of the fuel mass has been burnt.

Spray parameters

An example of images obtained from the Schlieren set-up in the case of PRF80 is presented in Figure 5 in inert and reactive ambient conditions. From the contour of the spray images, the penetration length S is calculated as indicated in ECN. Figure 6 shows an example of the evolution of the liquid and vapour spray penetration lengths for PRF80: the green curves are for one condition; the red one is an average of 6 tests and the black one the average +/- the standard deviation. The plot proves that the experiments done in NOSE setup are with a good repeatability as the standard deviation is less than 3%. Therefore, only the average values of the results are given below.

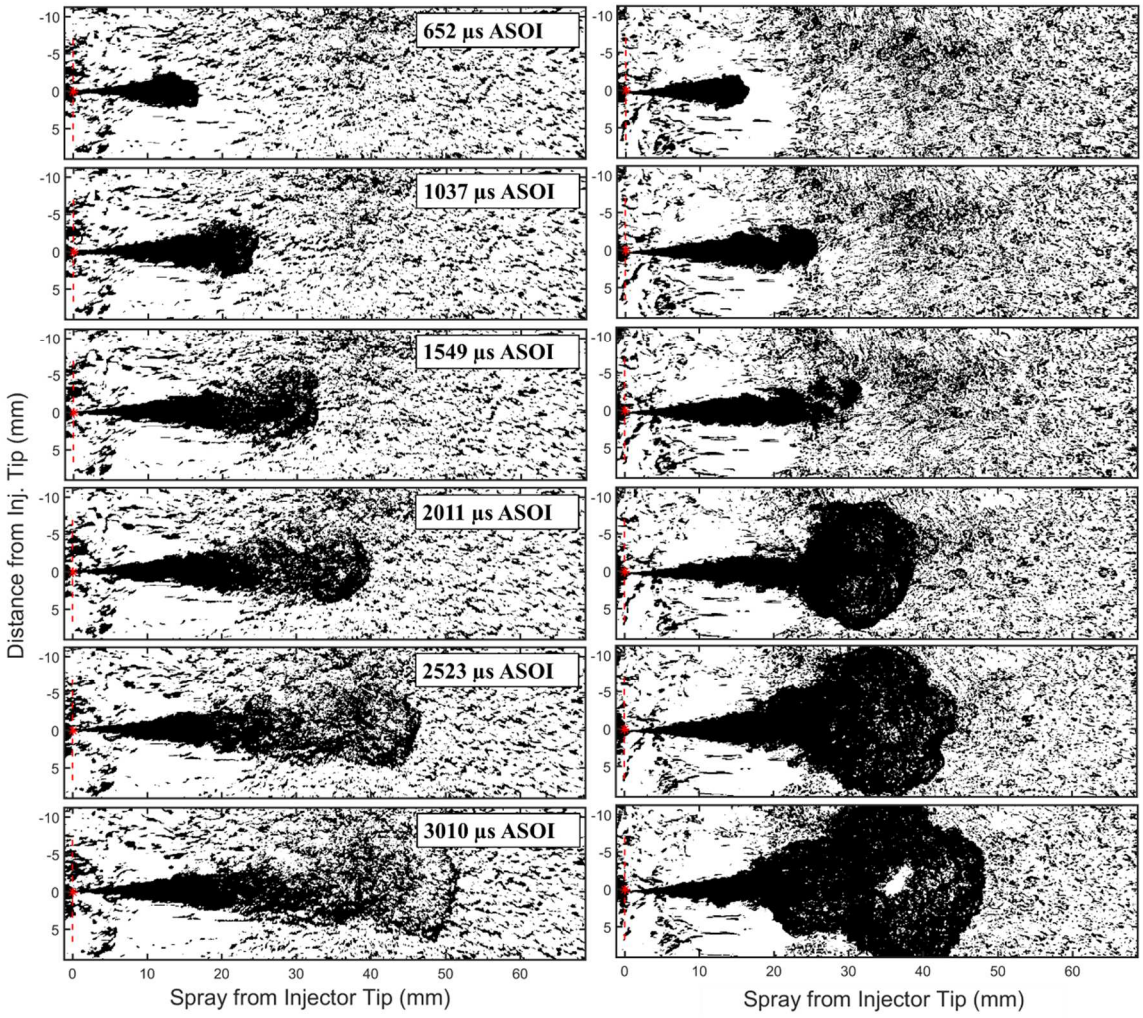

Figure 5. Schlieren images of spray with inert (left) and reactive (right) atmosphere

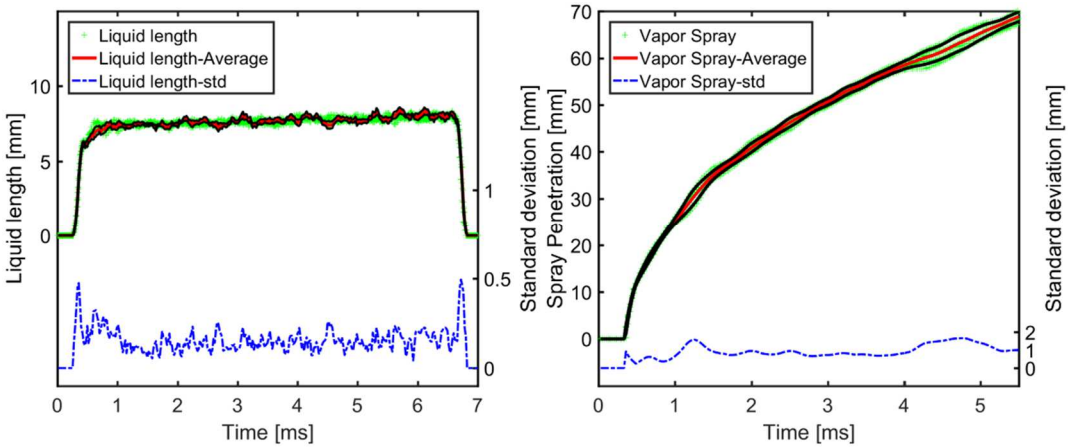

Figure 6. Evolution of the liquid and vapor spray penetration length of PRF80 with time

Combustion parameters

To determine the Lift-off-length, the approach suggested by Siebers and Higgins [29] was used. Once the combustion image has been filtered with a 3x3 pixel mean filter, the flame is divided through the axis defined from the injector tip into two profiles, a bottom and a top profile (Figure 7). The lift-off length is estimated by plotting the OH* intensity profile from the

injector tip for both the upper and lower axis. The values reported in this work were calculated with a 50% intensity peak, following the same criteria as Benajes et al. in [30].

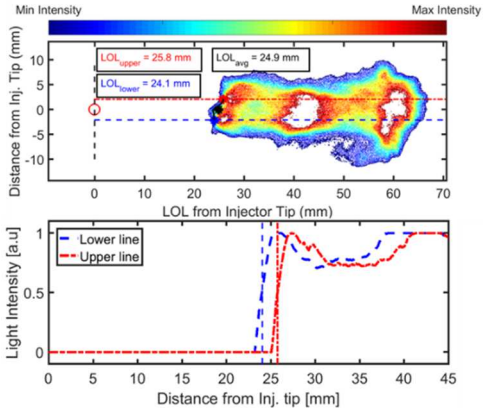

Figure 7. Flame Lift off length obtained by OH chemiluminescence: Top: example of one image. Bottom: intensity profiles for bottom (continuous red) and top (continuous blue) flame sections; dashed lines in the same colours represent LOL estimated with a 50% intensity peak*

3. Results

3.1 Effect of butanol quantity on spray processes

Figure 8 shows the temporal evolution of average vapor and liquid spray penetration lengths in non-reactive conditions for all fuels. First, for all the fuels tested, the liquid spray reaches a stable penetration length 0.5 ms after the start of injection (corrected by the hydraulic delay). But the liquid phase penetration length is strongly affected by the butanol content in the fuel, due to its higher viscosity and density. Figure 9 highlights the non-linear effect of butanol content on the liquid spray penetration length, determined during the stable phase of spray penetration: (1 to 1.5 ms): the effect is greater, i.e. higher gradient when the quantity of butanol is above 20% in volume. Therefore, as seen in Figure 8, the difference relative to the liquid length of PRF80 can reach 30% when 60% of butanol in vol. is added while the difference is only 5% with 20% of butanol. This result is extremely relevant in the context of partially premixed combustion strategies as the start of injection is significantly advanced compared to the Conventional Diesel Combustion mode, and can generate liquid fuel wall impingement.

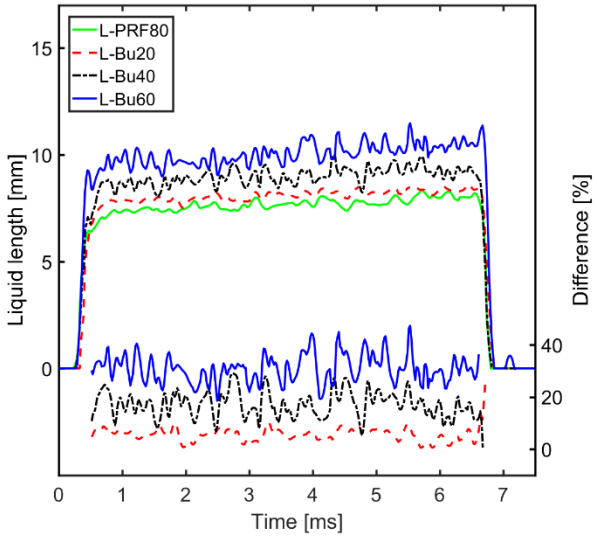

208

209 *Figure 8. Liquid Spray penetration of PRF80 and PRF80-Butanol blends – P_{amb} = 60 bar, T_{amb} = 900 K, P_{inj} = 400 bar.*

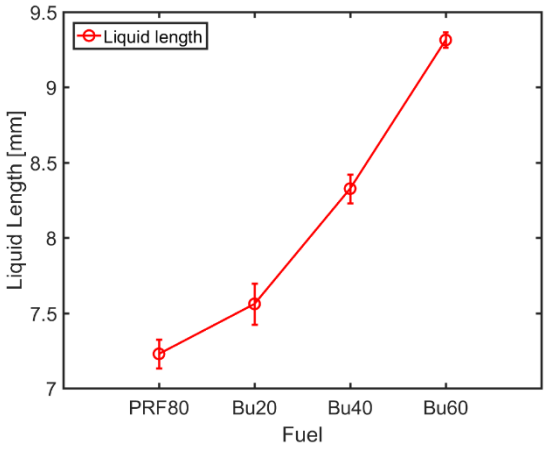

210

211 *Figure 9. Liquid length of PRF80 and PRF80 - n-butanol blends*

212 *P_{amb} = 60 bar, T_{amb} = 900 K, P_{inj} = 400 bar.*

213 The liquid penetration length was estimated from fuel properties, as the correlation suggested by Naber and Siebers

214 [31]:

215 $$LL = A.\sqrt{\frac{\rho_f}{\rho_{amb}}}.\frac{\sqrt{C_d}.d_{noz}}{\tan(\theta/2)}F(B) \text{ with } F(B) = \sqrt{\left(\frac{2}{B\left(P_{amb},T_{amb},T_f\right)}+1\right)^2 - 1} \quad \text{Eq. 2}$$

216 With A an arbitrary constant, $\frac{\rho_f}{\rho_{amb}}$ the fuel/air density ratio, C_d the discharge coefficient, d_{noz} the orifice diameter, θ the

217 angle spray and B, a term analogous the mass and thermal transfer number used in droplet vaporization studies, function of the

218 fuel properties (P_v, M_f, c_{pf}, L_v), ambient gas properties (M_a, c_p) and the operating conditions (P_{amb}, T_{amb}, T_f). Due to the multi

219 components of the fuel, to evaluate the effect of the n-butanol content on LL, the ratio F_{blend}/F_{PRF} was estimated by comparing

ratio LL_{blend}/LL_{PRF80} and $\sqrt{\frac{\rho_{blend}}{\rho_{PRF80}}}\sqrt{\frac{C_{d-blend}}{C_{d-PRF80}}}$, as the angle spray values for all fuels under steady state, i.e. from 1 to 1.5 ms, are around 21° ± 2° without any effect of butanol contents. With PRF80 and Bu60, $LL_{Bu60}/LL_{PRF80}=1.3$ and $\sqrt{\frac{\rho_{Bu60}}{\rho_{PRF80}}}\sqrt{\frac{C_{d-Bu60}}{C_{d-PRF80}}}=1.047$.

Addition, as reference as [32], the authors a correlation taking account fluid-mechanics with density and evaporative properties with temperature at which 50% of the fuel distilled in absence of specific and latent heat : $LL \propto d_{noz}^{a}.T_{amb}^{b}.P_{inj}^{c}.\rho_{f}^{e}.T_{50\%}^{h}$, with d_{noz} the orifice diameter, T_a the ambient gas temperature, P_{inj} the injection pressure, ρ_a ambient gas density, ρ_f the fuel density, $T_{50\%}$. But as it can be seen, in Table 3, the addition of butanol in gasoline blends has a very slight effect on distillation temperatures (extracted) from [33] . In fact, as underlined Dernotte et al. [34], the main change of liquid length is due to the high latent heat of vaporization, so for fuels like oxygenate fuels, the use of atmospheric pressure boiling point to correlate the liquid length is not sufficient.

Table 3. Distillation temperature of Gasoline and blends with n-butanol

Fuel	Gasoline	Bu20	Bu40	Bu60
$T_{10\%}$ [°C]	73 ± 0	74 ± 1	79 ± 1	88 ± 1
$T_{50\%}$ [°C]	105 ± 0	96 ± 0	97 ± 1	101 ± 0
$T_{90\%}$ [°C]	153 ± 5	135 ± 4	110 ± 2	106 ± 0

The specific heat considers as required heat to increase temperature until gases vapor condition: the heat transfer in term conduction from gas ambient to drops of spray. But, the latent heat as the amount of heat released during change of state from drops of spray to gases vaporization. The volatility as the mass transfer in term evaporation from drops spray to gases vaporization. The experimental results show that LL of Bu60 is the highest, that can be explain by higher: the specific heat (c_{pf}), boiling point temperature and the latent heat (L_v) and by lower vapor pressure due to require more heat of gas ambient transfer to drops spray for increase temperature of drops spray and until boiling point condition, and more heat released to evaporation. The evolution of LL as a function of Butanol contents is important to consider as function of the injection strategies for GPPC (one injection, multiple injection, injection phasing) the liquid fuel wall impingement can occur for high butanol quantity.

However, as can be noted in Figure 10, the vapor phase penetration length is very weakly affected by the butanol content: less than 3% of relative difference was observed, even with 60% butanol in volume.

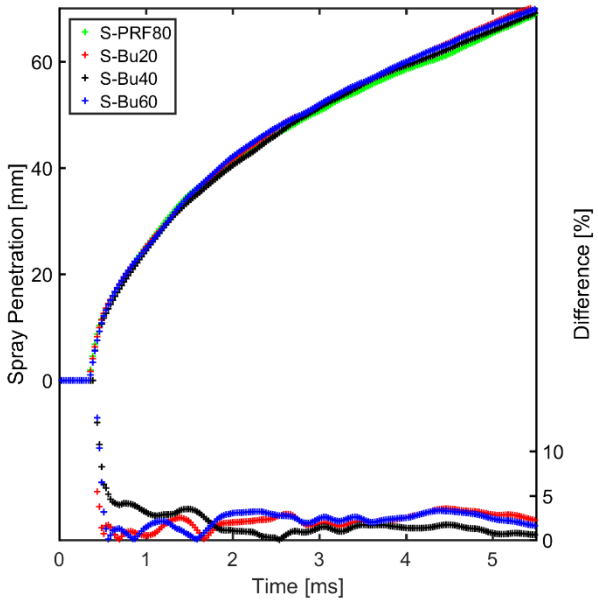

Figure 10. Vapor Spray penetration of PRF80 and PRF80-Butanol blends – P_{amb} = 60 bar, T_{amb} = 900 K, P_{inj} = 400bar.

3.2 Auto-ignition delays from kinetics modelling

The kinetics simulations were carried out using the constant volume model in the Senkin code [35]. The kinetics model for the blends was designed by using the 1033 species and 4238 reactions detailed mechanism proposed by Curran et al. [36] for the oxidation of iso-octane. This kinetics scheme based on the oxidation of n-heptane [37] can also be used for PRF oxidation. The oxidation of butanol was taken from the kinetic mechanisms of butanol isomers investigated by Sarathy et al. [38].

As the ambient temperature (at the injection timing, i.e. 900 K) is reduced during the vaporization process, the initial conditions for the simulations were set to 60 bar, with a temperature range from 790 K to 910 K, and due to the mixture fraction distribution, a wide equivalence ratio range from 0.2 to 2.0. These variations were explored to further describe the impact of n-butanol on PRF80 blends.

Figure 11 presents the iso-contour of the computed ignition delays for each fuel is plotted for all temperature and equivalence ratio ranges. As expected the ID increases with the increase of Butanol. So, at one given temperature, the same ignition delay can be reached for a higher equivalence ratio. For example, at 860 K, a 1 ms ignition delay is reached for an equivalence ratio of 1.5, 1.62, 1.9 and higher than 2 for a butanol content of 0, 20, 40 and 60% respectively. Therefore, the experimental measurements of the ignition delays associated with this map can provide an idea about the local equivalence ratio and temperature.

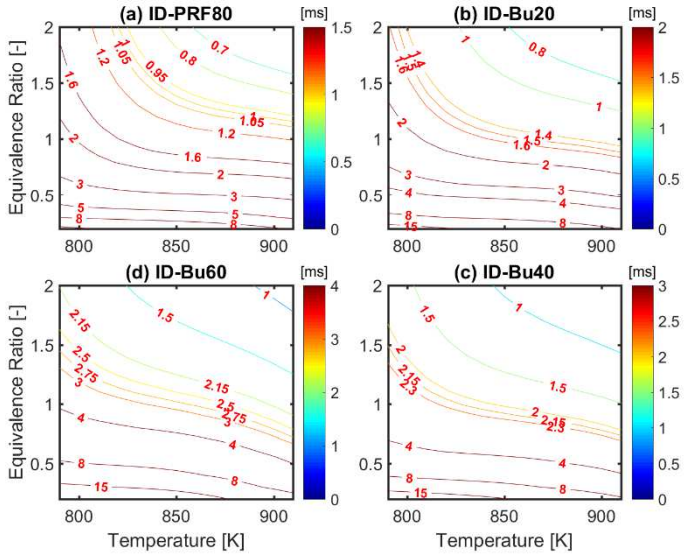

Figure 11. Ignition delay iso-contours for all fuels as a function of the temperature and equivalence ratio - P_{amb} = 60 bar.

The adiabatic temperature of the fuel/air mixture inside the chamber can described by:

$$m_a c_{pa}(T_m - T_{amb}) + m_f .L_v + m_f c_{pf}(T_m - T_b) = 0 \qquad \text{Eq. 3}$$

Here m_a, m_f: the mass of air inside the chamber and the mass of fuel injected, respectively, c_{pa}, c_{pf}: the heat capacity of air and fuel, respectively, L_v: the heating vapor of fuel, T_m, T_{amb}, T_b: Temperature of the air/fuel mixture, of the ambient gas and of the fuel boiling point, respectively. The temperature of the air/fuel mixture is expressed as:

$$T_m = \frac{c_{pa}T_{amb} + \frac{\theta}{\theta_{st}} c_{pf} T_b - \frac{\theta}{\theta_{st}} L_v}{c_{pa} + \frac{\theta}{\theta_{st}} c_{pf}}$$

The cooling effect of the fuel spray is considered in order to calculate the ignition delay as a function of the equivalence ratio. Indeed, for each air-fuel mixture, the initial adiabatic temperature can be calculated and used to determine the adiabatic temperature evolution during combustion. As, depending on the equivalence ratio, the initial mixture temperature depends on the physical properties of the fuel (such as boiling point, heat capacities and latent heat of vaporization), the initial mixture temperature set to estimate the ignition delay changes considerably as a function of the equivalence ratio and of the fuel. In Figure 12, the ignition delay is plotted by considering the 'adjusted' initial temperature as a function of the equivalence ratio for PRF80 and butanol blends. The trend is identical for all fuels: the ignition delay reaches a minimum value for an equivalence ratio between 1.2 and 1.5 before increasing again. As can be seen, the improvement in reactivity caused by the richer mixture competes with the lower mixture air-fuel temperature due to the cooling effect associated with higher fuel concentrations. For lean conditions with ER < 1.2, the ignition delay time decreases while the equivalence ratio increases, in

contrast to the rich condition with ER > 1.5 caused by the cooling effect associated with the stronger increase in fuel molar fractions. The minimum in ignition delay time corresponds to the best reactive combination between equivalence ratio and initial mixture temperature. As expected, Figure 12 shows that for a given ER, a higher n-butanol concentration shortens the ignition delay. Therefore, the effect of butanol content is higher: for 60% of n-butanol content and the ignition delay is twice as long.

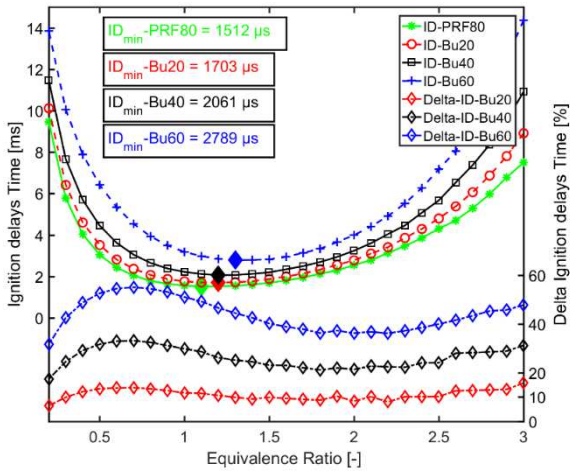

Figure 12. Ignition delay as a function of equivalence ratio for PRF80/Bu blendsas under adiabatic corresponding temperature, 'bright' losanges indicate minimum ignition delay for each fuel - P_{amb} = 60 bar.

3.3 Effect of butanol quantity on combustion processes

In Figure 13, the evolution of the average pressure in the combustion chamber and the average apparent heat release rate are plotted versus time. It can be seen that the start of combustion occurs at least 1.5 ms after the start of injection, so in a region where the vapor spray penetration is far from the liquid penetration as confirmed in from Figure 6 second it has to be noted that as a function of the increase in Butanol content, the combustion onset is strongly delayed, due to both the difference in the chemical ignition delay but also the vaporization and mixing processes in HP/HT vessel.

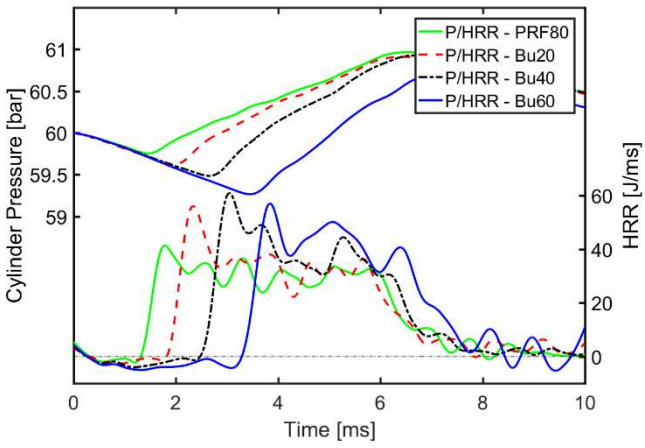

Figure 13. Typical pressure and Heat release rates - P_{amb} = 60 bar, T_{amb} = 900 K, P_{inj} = 400 bar.

Figure 14 illustrates the experimental ID of all the fuels obtained from OH* chemiluminescence intensity and HRR

temporal evolutions. Both estimates, averaged over the 6 experimental tests are overall in a very good agreement. ID values, obtained for a stoichiometric mixture at 900 K and the values obtained from Figure 12, i.e. the minimum ones determined previously from kinetics simulation are also plotted. Even if the estimate of the initial temperature (by taking into account the cooling effect due to the latent vaporization heat) is rough with the simple equation, globally a good agreement is obtained.

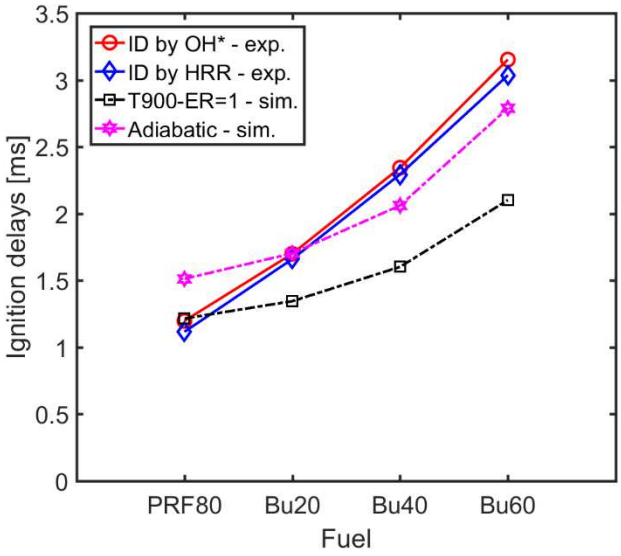

Figure 14. Average Ignition delay: experimental and simulated estimates for all fuels - P_{amb} = 60 bar, T_{amb} = 900 K, P_{inj} = 400 bar.

From Figure 13 also, the shape of the HRR indicates a combustion process in two phases: the premixed phase and the mixing controlled phase (i.e. diffusion phase).as the fuel is a gasoline type, these two phases are less easily distinguishable than for diesel fuel. Indeed, the combustion process itself is a mix between premixed and mixing controlled combustion modes. The first peak seems to be more important as a function of the butanol amount increase To confirm that, the different phases of the combustion process (i.e. time for 10, 50 and 90 % of the fuel mass fraction to be burnt, BMF10, BMF50, BMF90 respectively) and the global combustion duration (BMF90-BMF10), split in two phases (BMF50-BMF10, and BMF90-BMF50) were estimated and are plotted in Figure 15.

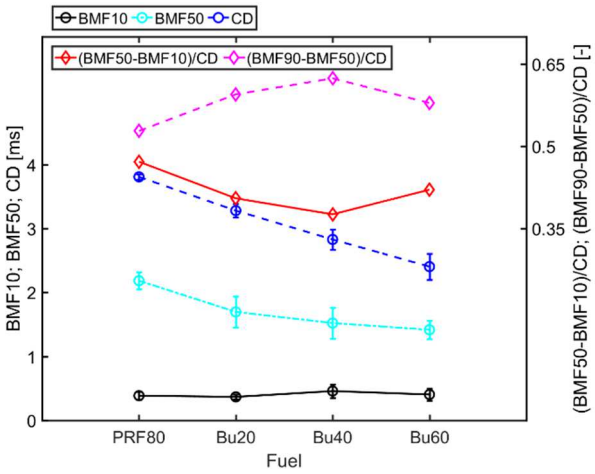

Figure 15. Different combustion phases for all fuels - P_{amb} = 60 bar, T_{amb} = 900 K, P_{inj} = 400 bar

The earlier stage of combustion is slightly increased as a function of butanol content but the decrease of BMF50 indicates that combustion is faster with butanol, as can be predicted from the laminar flame velocity measurements [39]. It is interesting to note that also the total burning time decreases linearly with the n-butanol amount in the blend. Due to the longer ignition delay, the increase of butanol in the blend favors the premixing of fuel and air. But by considering the both half part of the combustion It can be noted that even if the global effect of butanol addition is linear if only the temporal evolution of the combustion is considered (BMF50, CD) the effect of butanol content is not linear, it is to say that when the amount of butanol is higher than 50%, the premixed phase duration is longer due to the difference of vaporisation physical parameters of butanol in comparison to PRF80.

From OH* chemiluminescence images, it is possible to determine the evolution of the global Averaged Spatially integrated Intensity, as $ASI = \frac{\sum_i \sum_j I_{i,j}}{N}$, with $I_{i,j}$ the intensity at pixel position (i, j) and N the total pixel number. The plot of *ASI* versus time, as Figure 16, helps to identify the premixed phase. Indeed, the rank is similar to the ID rank: PRF80 ASI starts the first, followed by butanol blends as a function of the butanol amount as already observed from the heat release rate plot in Figure 13.

However, ASI is more sensitive to the n-butanol concentration: the peak decreases with the increase in butanol and the time duration also, confirming the shorter combustion duration of the premixed combustion phase.

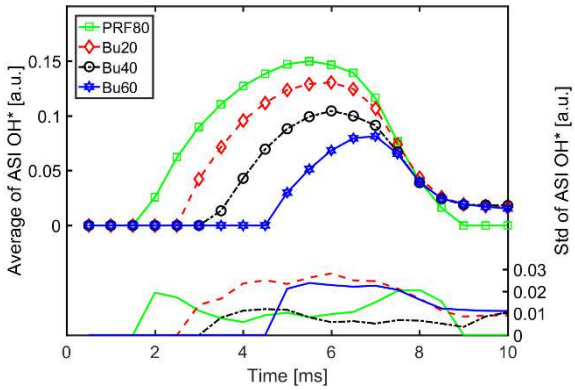

Figure 16. Averaged spatially integrated of Flame OH - P_{amb} = 60 bar, T_{amb} = 900 K, P_{inj} = 400 bar*

3.4 Effect of butanol amount on Lift off Length

Flame lift-off length (LOL) is an indicator of the mixing time between air and fuel before the ignition which induces the combustion and pollutant process. The temporal evolution of lift off length for PRF80 and n-butanol blends is plotted in Figure 17. It can be noted that the flame first stabilizes far from the injector tip and then slowly approaches it. These movement can be explained by a variation of average ambient temperature during the combustion. As the NOSE volume is smaller this effect is no-negligible. When the fuel injection is stopped, i.e. at 6.5 ms, the flame is convected by the vapor spray. The combustion process continues for a quite a long time after the end of injection, though in a narrower combustion region. Compared with the liquid penetration length evolution, the higher value of LOL proves that fuel reaches the combustion region after total vaporization and that the fuel vapor continues to move downstream with the air entrainment. Then, the fuel vapor and air mixture reaches the reaction zone and is ignited by the flame. Due to the strong effect of containment, the LOL is stable in a relatively small temporal range, identified in Figure 17 by the black symbols.

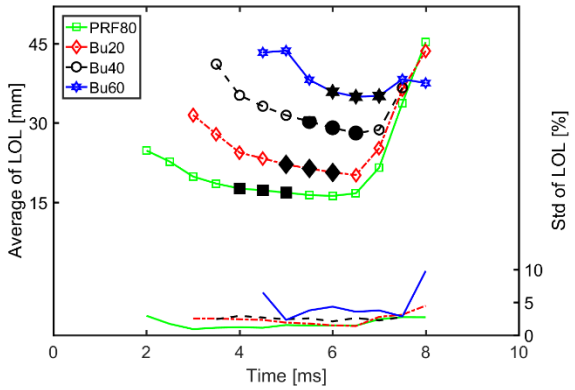

Figure 17. Temporal evolution of Flame Lift off for all fuel conditions - P_{amb} = 60 bar, T_{amb} = 900 K, P_{inj} = 400 bar

As reminded Benajes et al. in [30], the Lift off length is strongly related to gas-jet theory as: $LOL \propto T_{amb}^{a}.\rho_{amb}^{b}.u_{th}^{c}.O_{2\%}^{d}$, with u_{th} the theoretical velocity of the fuel at the orifice outlet, $u_{th} = \sqrt{2(\Delta p_{noz} / \rho_f)}$, Δp_{noz} the pressure drop through the nozzle orifice approximated to (p_{rail} - p_{amb}) and *a, b, c, d* constant. As in this present study, all parameters were set constant,

345 only fuels change.

346 Therefore, the LOL has to be mainly dependant on the fuel density as: $\frac{LOL_{blend}}{LOL_{PRF80}} = \left(\sqrt{\frac{\rho_{PRF80}}{\rho_{blend}}} \right)^{c}$. But contrary to the results

347 predicted by Benajes et al. [30], the constant exponent, c as presented in Figure 18, is negative, indicating certainly that this
348 other parameters have to be taking into account in the case of gasoline and alcohols fuels . Indeed, as underlined by [24,40,41],
349 the LOL is not only affected by the spray feature but also by the oxygen content in the fuel due to the induced change of the
350 stoichiometric mixture fraction Z_{st}. The evolution of the Lift off length as a function of the stoichiometric air-fuel ratio is

351 presented also in Figure 18 as $\frac{LOL_{blend}}{LOL_{PRF80}} = \left(\frac{AFR_{blend}}{AFR_{PRF80}} \right)^{e}$ with AFR the air fuel ratio stoichiometric. The similar evolution

352 indicates that both parameters, density and air/fuel ratio have identical weight.

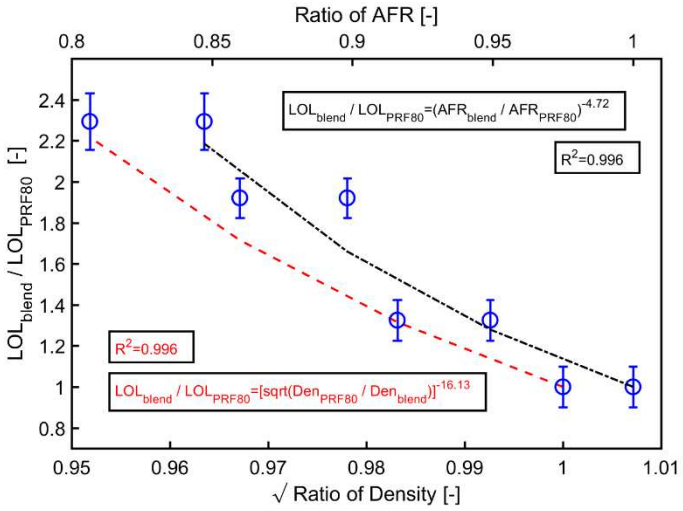

353

354 *Figure 18. Measured lift off length versus the density and the stoichiometric air-fuel ratio for butanol blends relative to*
355 *values for PRF80*

356 Another way LOL is related with ignition delay [42]. It is described by the Arrhenius-type law. Last, the linear
357 relationship between LOL and ID is observed in most studies [26], especially focused on Diesel type fuel. The evolution of the
358 lift off length or ignition delay versus the Octane Number are plotted Figure 19. The estimates of ID by OH*
359 chemiluminescence and LOL, presented in Figure 14 and Figure 17 respectively are also plotted.
360 The linear dependency between ID and RON or LOL and RON is well observed. The ignition delay is more sensitive to ratio
361 of octane number.

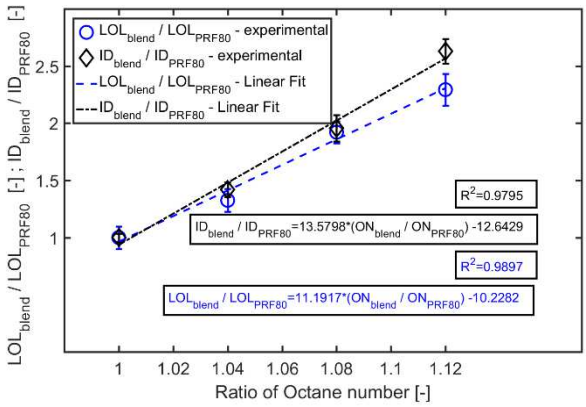

Figure 19. Lift off length and ignition delay ratios as a function of octane number ratio for all fuels. Data compiled from Figure 14 and 17

4. Conclusions

For the first time, experiments were carried out to explore the mixing and the auto-ignition processes in GCI mode under high temperature and high pressure conditions in the case of gasoline surrogate (PRF80) and n-butanol blends in order to consider bio-butanol blends as potential renewable fuels for Gasoline Compression Ignition engine for the first time in a dedicated set-up. .

The main conclusions of the work are as follows:

- **Under inert atmosphere conditions,** the addition of n-butanol affects the liquid spray until 35% for the highest content of 60% in volume but without real impact on the vapor spray penetration evolution.
- **Under reactive atmosphere conditions,** as the increase of n-butanol content in the mixture decreases drastically the reactivity of the mixture, the combustion is delayed and located further from the nozzle, as indicated the ignition delay and flame lift-off length evolution as a function of blends. The main results can be summarized as by increasing the amount of n-butanol in the mixture results:
    - Increases the flame lift-off length which leads to decreasing the local equivalence ratio in the combustion region, resulting in lower soot formation.
    - Results in shorter combustion duration and relatively strongly premixed combustion.

Therefore, butanol addition in gasoline could be a good solution in GCI combustion mode as it allows the adjustment of the combustion phasing and its optimisation in engine to increase the efficiency.

Acknowledgements

The authors acknowledge the Ministry of Education and Training of Vietnam for financing the Ph. D of Tung Lam Nguyen at the University of Orleans and the French National Research Agency (contract ANR-14-CE22-0015-01) for financial support to the ECN-France project and Region Centre Val de Loire (CPER 2007-2013 Energies du Futur) and FEDER for

financial support to build the experimental set-up.

References

[1] Zheng P, Allen WB, Roesler K, Williams ME, Zhang S, Li J, et al. Metabolic engineering delivers next-generation biofuels. Nat Genet 2008;40:367–72. doi:10.1038/ng.85.

[2] Kalghatgi G, Hildingsson L, Johansson B. Low NOx and Low Smoke Operation of a Diesel Engine Using Gasolinelike Fuels. ASME 2009 Intern Combust Engine Div Spring Tech Conf 2009:259–71. doi:10.1115/ICES2009-76034.

[3] Rezaei SZ, Zhang F, Xu H, Ghafourian A, Herreros JM, Shuai S. Investigation of two-stage split-injection strategies for a Dieseline fuelled PPCI engine. Fuel 2013;107:299–308. doi:10.1016/j.fuel.2012.11.048.

[4] Manente V, Zander C-G, Johansson B, Tunestal P, Cannella W. An Advanced Internal Combustion Engine Concept for Low Emissions and High Efficiency from Idle to Max Load Using Gasoline Partially Premixed Combustion. SAE Tech. Pap. Ser., 2010. doi:10.4271/2010-01-2198.

[5] Manente V, Johansson B, Tunestal P, Sonder M, Serra S. Gasoline partially premixed combustion: high efficiency, low NOx and low soot by using an advanced combustion strategy and a compression ignition engine. Int J Veh Des 2012. doi:10.1504/ijvd.2012.048689.

[6] Sellnau M, Foster M, Hoyer K, Moore W, Sinnamon J, Husted H. Development of a Gasoline Direct Injection Compression Ignition (GDCI) Engine. SAE Int J Engines 2014;7:835–51. doi:10.4271/2014-01-1300.

[7] Rousselle CM, Foucher F, Labreche A. Optimization of Gasoline Partially Premixed Combustion Mode. SAE Tech. Pap. Ser., SAE International; 2013. doi:10.4271/2013-01-2532.

[8] Dempsey AB, Curran SJ, Wagner RM. A perspective on the range of gasoline compression ignition combustion strategies for high engine efficiency and low NOx and soot emissions: Effects of in-cylinder fuel stratification. Int J Engine Res 2016. doi:10.1177/1468087415621805.

[9] Labreche A, Foucher F, Rousselle C. Impact of the Second Injection Characteristics and Dilution Effect on Gasoline Partially Premixed Combustion. SAE Tech. Pap. Ser., 2014. doi:10.4271/2014-01-2673.

[10] Pinazzi PM, Foucher F. Influence of injection parameters, ozone seeding and residual NO on a Gasoline Compression Ignition (GCI) engine at low load. Proc Combust Inst 2017;36:3659–68. doi:10.1016/j.proci.2016.06.075.

[11] Manente V, Johansson B, Tunestal P, Cannella W. Effects of Different Type of Gasoline Fuels on Heavy Duty Partially Premixed Combustion. SAE Int J Engines 2009;2:71–88. doi:10.4271/2009-01-2668.

[12] Cung KD, Ciatti SA, Tanov S, Andersson Ö. Low-Temperature Combustion of High Octane Fuels in a Gasoline Compression Ignition Engine. Front Mech Eng 2017;3:1–14. doi:10.3389/fmech.2017.00022.

[13] Manente V, Tunestal P, Johansson B, Cannella WJ. Effects of Ethanol and Different Type of Gasoline Fuels on

Partially Premixed Combustion from Low to High Load. SAE Tech. Pap. Ser., 2010. doi:10.4271/2010-01-0871.

[14] Woo C, Goyal H, Kook S, Hawkes ER, Chan QN. Double Injection Strategies for Ethanol-Fuelled Gasoline Compression Ignition (GCI) Combustion in a Single-Cylinder Light-Duty Diesel Engine. SAE Tech. Pap. Ser., SAE International; 2016. doi:10.4271/2016-01-2303.

[15] Shamun S, Shen M, Johansson B, Tuner M, Pagels J, Gudmundsson A, et al. Exhaust PM Emissions Analysis of Alcohol Fueled Heavy-Duty Engine Utilizing PPC. SAE Int J Engines 2016;9:2142–52. doi:10.4271/2016-01-2288.

[16] Kaiadi M, Johansson B, Lundgren M, Gaynor JA. Experimental Investigation on different Injection Strategies for Ethanol Partially Premixed Combustion. SAE Tech. Pap. Ser., SAE International; 2013. doi:10.4271/2013-01-0281.

[17] Noh HK, No S. Effect of bioethanol on combustion and emissions in advanced CI engines : HCCI , PPC and GCI mode – A review 2017. doi:10.1016/j.apenergy.2017.09.071.

[18] Han X, Zheng M, Wang J. Fuel suitability for low temperature combustion in compression ignition engines. Fuel 2013;109:336–49. doi:10.1016/j.fuel.2013.01.049.

[19] Yang B, Yao M, Cheng WK, Zheng Z, Yue L. Regulated and unregulated emissions from a compression ignition engine under low temperature combustion fuelled with gasoline and n-butanol/gasoline blends. Fuel 2014;120:163–70. doi:10.1016/j.fuel.2013.11.058.

[20] Baumgardner ME, Sarathy SM, Marchese AJ. Autoignition characterization of primary reference fuels and n-heptane/n-butanol mixtures in a constant volume combustion device and homogeneous charge compression ignition engine. Energy and Fuels 2013;27:7778–89. doi:10.1021/ef4015982.

[21] AlRamadan AS, Badra J, Javed T, Al-Abbad M, Bokhumseen N, Gaillard P, et al. Mixed butanols addition to gasoline surrogates: Shock tube ignition delay time measurements and chemical kinetic modeling. Combust Flame 2015;162:3971–9. doi:10.1016/j.combustflame.2015.07.035.

[22] Gorbatenko I, Tomlin AS, Lawes M, Cracknell RF. Experimental and modelling study of the impacts of n-butanol blending on the auto-ignition behaviour of gasoline and its surrogate at low temperatures. Proc Combust Inst 2019. doi:10.1016/j.proci.2018.05.089.

[23] López JJ, García-Oliver JM, García A, Domenech V. Gasoline effects on spray characteristics, mixing and auto-ignition processes in a CI engine under Partially Premixed Combustion conditions. Appl Therm Eng 2014;70:996–1006. doi:10.1016/j.applthermaleng.2014.06.027.

[24] Nilaphai O, Hespel C, Chanchaona S, Mounaïm-Rousselle C. Spray and Combustion Characterizations of ABE/Dodecane Blend in Comparison to Alcohol/Dodecane Blends at High-Pressure and High-Temperature Conditions. Fuel 2018;225:542–53. doi:10.1016/j.fuel.2018.03.184.

[25] Nilaphai O. Vaporization and Combustion Processes of Alcohols and Acetone-Butanol-Ethanol (ABE) blended in n-Dodecane for High Pressure-High Temperature Conditions. Orleans, 2019.

[26] Anderson JE, Kramer U, Mueller SA, Wallington TJ. Octane numbers of ethanol- and methanol-gasoline blends estimated from molar concentrations. Energy and Fuels 2010;24:6576–85. doi:10.1021/ef101125c.

[27] Anderson JE, Dicicco DM, Ginder JM, Kramer U, Leone TG, Raney-Pablo HE, et al. High octane number ethanol-gasoline blends: Quantifying the potential benefits in the United States. Fuel 2012;97:585–94. doi:10.1016/j.fuel.2012.03.017.

[28] Hayes TK, Savage LD, Sorenson SC. Cylinder Pressure Data Acquisition and Heat Release Analysis on a Personal Computer. SAE Tech. Pap. Ser., 1986. doi:10.4271/860029.

[29] Siebers DL, Higgins B. Flame Lift-Off on Direct-Injection Diesel Sprays Under Quiescent Conditions 2001. doi:10.4271/2001-01-0530.

[30] Benajes J, Payri R, Bardi M, Martí-Aldaraví P. Experimental characterization of diesel ignition and lift-off length using a single-hole ECN injector. Appl Therm Eng 2013;58:554–63. doi:10.1016/j.applthermaleng.2013.04.044.

[31] Siebers DL. Scaling Liquid-Phase Fuel Penetration in Diesel Sprays Based on Mixing-Limited Vaporization. SAE Tech. Pap. Ser., vol. 1, 2010. doi:10.4271/1999-01-0528.

[32] Pastor J V., García-Oliver JM, Nerva JG, Giménez B. Fuel effect on the liquid-phase penetration of an evaporating spray under transient diesel-like conditions. Fuel 2011;90:3369–81. doi:10.1016/j.fuel.2011.05.006.

[33] Aghahossein Shirazi S, Abdollahipoor B, Martinson J, Windom B, Foust TD, Reardon KF. Effects of dual-alcohol gasoline blends on physiochemical properties and volatility behavior. Fuel 2019;252:542–52. doi:10.1016/j.fuel.2019.04.105.

[34] Mounaïm-Rousselle C, Dernotte J, Foucher F, Hespel C, Houille S. Influence of the fuel properties on the spray development characteristics in a Diesel optical access engine. 10th Int. Symp. Combust. Diagnostics, 2012.

[35] Chemkin. Senkin: a fortran program for predicting homogeneous gas phase chemical kinetics with sensitivity analysis. Sci York 1987.

[36] Curran HJ, Gaffuri P, Pitz WJ, Westbrook CK. A comprehensive modeling study of iso-octane oxidation. Combust Flame 2002. doi:10.1016/S0010-2180(01)00373-X.

[37] Curran HJ, Gaffuri P, Pitz WJ, Westbrook CK. A comprehensive modeling study of n-heptane oxidation. Combust Flame 1998. doi:10.1016/S0010-2180(97)00282-4.

[38] Sarathy SM, Vranckx S, Yasunaga K, Mehl M, Oßwald P, Metcalfe WK, et al. A comprehensive chemical kinetic combustion model for the four butanol isomers. Combust Flame 2012;159:2028–55.

doi:10.1016/j.combustflame.2011.12.017.

[39] Broustail G, Seers P, Halter F, Moréac G, Mounaim-Rousselle C. Experimental determination of laminar burning velocity for butanol and ethanol iso-octane blends. Fuel 2011. doi:10.1016/j.fuel.2010.09.021.

[40] Donkerbroek AJ, Boot MD, Luijten CCM, Dam NJ, ter Meulen JJ. Flame lift-off length and soot production of oxygenated fuels in relation with ignition delay in a DI heavy-duty diesel engine. Combust Flame 2011;158:525–38. doi:10.1016/j.combustflame.2010.10.003.

[41] Manin J, Skeen S, Pickett L, Kurtz E, Anderson JE. Effects of Oxygenated Fuels on Combustion and Soot Formation/Oxidation Processes. SAE Int J Fuels Lubr 2014;7:704–17. doi:10.4271/2014-01-2657.

[42] Pickett LM, Siebers DL, Idicheria CA. Relationship Between Ignition Processes and the Lift-Off Length of Diesel Fuel Jets. SAE Tech. Pap. Ser., SAE International; 2005. doi:10.4271/2005-01-3843.

Nomenclature

Acronyms

AFR	Stoichiometric air-fuel ratio
ASOI	After start of injection
ASI	Averaged spatially integrated
Bu20	80% PRF80 / 20% n-Butanol by Volume
Bu40	60% PRF80 / 40% n-Butanol by Volume
Bu60	40% PRF80 / 60% n-Butanol by Volume
BMF10	Burnt mass fraction 10%
BMF50	Burnt mass fraction 50%
BMF90	Burnt mass fraction 90%
ECN	Engine Combustion Network
CD	Combustion duration
C_d	Discharge coefficient
CVC	Constant volume chamber
ER	Equivalence ratio
EGR	Exhaust gas recirculation
GCI	Gasoline compression ignition
HRR	Heat release rate

FIT	Fuel ignition tester
LTC	Low temperature combustion
MFR	Mass flow rate
IQT	Ignition quality tester
SOC	Start of combustion
SOI	Start of injection
PID	Proportional-Integral-Derivative controller
PPC	Partially premixed combustion
PRF	Primary Reference Fuel
RON	Research octane number
Variable	
c_p	Specific heat for an ideal gas at constant pressure
c_{pf}	Specific heat for an fuel vaporization at constant pressure
c_v	Specific heat for an ideal gas at constant volume
d_{noz}	Diameter
ID	Ignition delay time
k-factor	Conicity factor used in industry
LOL	Flame Lift off length
LL	Liquid spray penetration length
$\dot{m}_{me}$	Mean mass flow rate
$\dot{m}_{th}$	Theoretical mass flow rate
P	Pressure
V	Volume
R	Gas constant
Re	Reynolds number
S	Vapor spray penetration length
T	Temperature
t	Time
γ	Specific heat ratio
υ_f	Viscosity of fuel

537	ρ_f	Fuel density
538	θ	Angle spray